A Hydrodynamic Model of Cerebrospinal Fluid Flow in Man

Rolf Wüst, Trygve Kolberg, Alvaro Palma *, and Alfredo Palma **

Neurochirurgische Universitätsklinik (Direktor Prof. Dr. Dr. R. Wüllenweber), Sigmund-Freud-Straße 25, D-5300 Bonn/Venusberg

Z. Naturforsch. **35 c**, 326–339 (1980); received January 16, 1978/September 24, 1979

Cerebrospinal Fluid Dynamics, Hydrodynamic Bi-Compartmental Model, Mathematical Analysis, Cerebrospinal Fluid Flow Parameters, Radioisotope Serial Scanning

A hydrodynamic bi-compartmental model for the cerebrospinal fluid (CSF) flow in humans is presented which combines anatomical and physiological conditions in the central nervous system with results of special radioisotope diagnostic techniques. Normal and disturbed conditions, the diagnostic methods and the results are explained. A differential equation for the time behaviour of regional radioisotope concentrations is derived by applying to the model mathematical procedures which are familiar from the description of radioactive decay series, or reaction kinetics of chemical or pharmaceutical processes. The solutions are analysed and discussed with respect to findings of isotope diagnostics, and parameters for the complete and quantitative evaluation of CSF flow systems are derived. A system factor is introduced for classification purposes and, in conjunction with basic principles of hydrodynamics, is used to postulate a similarity law of CSF flow systems. The diagnostical and therapeutical value of the model for analysis and simulation of CSF flow systems is discussed. Practical applications to other disciplines are proposed.

1. Introduction

1.1 General methods

Different tissues or intracorporal fluids of the living body store certain substances (*e. g.* chemicals or pharmaceuticals) differently. *Scintigraphy*, a technique developed in the early 1950's for medical research and diagnostic purposes, exploits this effect and demonstrates the distribution patterns of such radioactively tagged substances by detecting the gamma radiation emitted [1].

Rapid sequential gamma camera scintigraphy (RSGCS) represents one of the most recent developments in scintigraphic techniques. As with the cinematographic recording of moving processes, a gamma scintillation camera, in conjunction with digital computer-aided acquisition and storage of data, samples in appropriate time intervals rapid frame sequences of the images of radionuclide distribution in areas of the human body for the study of dynamic processes [2, 3].

Each tracer distribution pattern is stored point-by-point in a digital matrix in which each element represents the tracer activity within a volume element of the examined region. Using the *"region of interest" (ROI)* technique, the time behaviour of tracer activity in selectable areas in the sequence of radionuclide images can be visualized in time-activity histograms or plots.

A *multichannel analyser system* subsequently displays the radionuclide images on a screen, and permits the delineation of interesting regions with a light pen. The analyser performs background and decay corrections, calculates the amount of total tracer activity in the ROI at that time point, and normalizes this value by the initial – and maximal – activity. This is the activity encountered in the tracered region immediately after tracer application. Plotting the values thus obtained point by point, with the time elapsed since the initial tracer injection as abscissa, yields a graph of *normalized regional tracer activity* versus time. The identical plot results for the *normalized tracer concentration* versus time independently of the applied activity because of the proportionality between tracer activity and tracer concentration. Details of instrumentation and procedures are given in [4] and [5].

Gammacisternography (GCG) and *gammaventriculography (GVG)* are two special scintigraphic meth-

---

* Permanent address: Instituto Neurocirugía, Santiago, Chile.
** Present address: BASF Quimica Colombiana S. A. Medellín, Colombia.

Abbreviations: CSF, cerebrospinal fluid; RSGCS, rapid sequential gamma camera scintigraphy; ROI, region of interest; GCG, gammacisternography; GVG, gammaventriculography; CVS, cerebral ventricular system; DA, distribution area; CVR, cisterno-ventricular reflux.

Reprint requests to R. Wüst.

0341-0382/80/0300-0326 $ 01.00/0

ods to examine neurological and neurosurgical syndromes caused by or associated with anatomical abnormalities inside the cranium with disturbances of the intracranial circulation of the *cerebrospinal fluid (CSF).*

1.2 Anatomical and physiological conditions

The brain, situated inside the skull, and the spinal cord, located inside the vertebral column, are both protected by meninges, and the interstices are filled with a clear, acqueous liquid, the CSF. CSF is also contained in four normally communicating cavities, the so – called ventricles, lying in the brain itself, which together form the *cerebral ventricular system (CVS).* This consists of the two lateral ventricles, which are located symmetrically in the forebrain hemispheres, and the third and fourth ventricles, which in turn lie below the lateral ventricles in the midline of the brain stem.

Another cavity filled with CSF, the *system of the basal cisterns,* is situated below and outside the brain at the base of the skull. As a functional unit, the cisternal system comprises all the basal cisterns together with the uppermost part of the spinal canal [4].

1.3 Scintigraphic results

The site, shape, and dimensions of the CVS can be determined with the help of GVG [5, 6], which is performed by introducing a radiotracer substance into one of the lateral ventricles via the anterior fontanelle or a trepan hole. In combination with RSGCS storage facilities, GVG allows the study of the CSF flow pathways in the CVS [5].

Under normal conditions – as far as is presently known [7–11] – the CSF is produced mainly in the two lateral ventricles. The route by which the CSF leaves the CVS leads from the third ventricle through the aquaeductus of Sylvii, into the fourth ventricle, and from there into the basal cisterns.

GCG is accomplished by injecting the radiotracer substance into the cisternal system by suboccipital puncture. In conjunction with computer-assisted data storage, GCG clarifies the routes of CSF elimination in the regions outside the brain and the resorption pathways of CSF [4, 11, 12].

The CSF descends from the cisternal system towards the spinal canal and also ascends into the CSF – filled spaces surrounding the brain convexity, the so-called *epicortical space.* Therefore, the cisternal system is understood to be a *distribution area (DA)* whose properties have already been discussed in detail [4, 12]. Finally, the CSF is resorbed principically in the upper area of the epicortical space.

1.4 The pathological cisterno-ventricular reflux

Pathological conditions can disturb CSF dynamics. In such cases, GCG shows that radiotracer injected into the DA reaches the CVS *against* the normal CSF current from the CVS to the DA. Though no real reversal of the CSF current in fact takes place [13], this phenomenon is often seen. It is referred to as *cisterno-ventricular reflux (CVR)* [5, 7, 8, 14, 15].

1.5 The origin of the hydrodynamic model

All these normal and pathological CSF flow conditions summarized above have been ascertained by or detected through the time behaviour of isotope concentrations observed in scintigraphic examinations. The analysis of temporal evolution of tracer concentrations in the CVS and DA, observed in GCG and GVG, lead us to postulate a simplified *hydrodynamic model of CSF flow* [5, 13].

Initial applications of this theoretical model to clinical cases explained the CVR as being induced by turbulence [5], and classified several stages in the development of hydrocephalus [16]. This paper analyses this model mathematically, and describes its theoretical aspects. Both the principles of fluid dynamics and mathematical solutions derived from the model, will be used to postulate intrinsic properties of CSF dynamics and define parameters for a quantitative evaluation of CSF flow.

2. Qualitative properties of the model

2.1 The volumes and the CSF flows

Anatomical and physiological conditions in human CSF dynamics are comparable to those of a *hydrodynamic system* consisting of two connected compartments, A and B, simulating CVS and DA respectively (Fig. 1). They contain the volumes V_A and V_B of a fluid and are linked by two pipes in which two independent fluid currents represent the physiological CSF flow V'_{AB}, from the CVS to the DA, and the pathological CSF reflux V'_{BA}, from the DA to the CVS. The prime "′" denotes the time

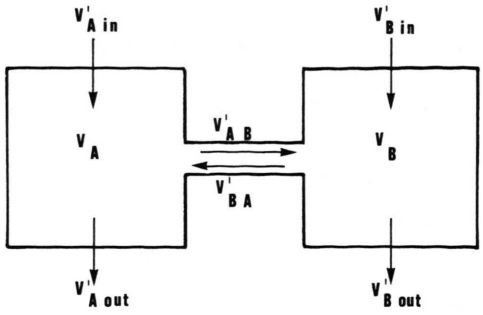

Fig. 1*. The hydrodynamic model.

derivative $V'_{AB} = dV_{AB}/dt$, where V_{AB} is the volume of fluid flowing from the CVS to the DA during a unit of time. The prime notation is used for all CSF flows and also for tracer concentration changes.

In order to illustrate all possible situations, each compartment is assumed to have both inflows and outflows for the simulation of CSF production, and resorption or outflow, respectively. An equilibrium between production and resorption is postulated in the model in order to avoid unnatural inflation or collapse of the system.

The CSF production in the CVS corresponds to an influx $V'_{A\,in}$. The smaller – in most cases negligible – amount of CSF production in the DA is denoted $V'_{B\,in}$. The leakage flow $V'_{A\,out}$ takes into account the transependymal resorption of CSF in the walls of the CVS, the amount of which, however, is significant only in cases of pronounced hydrocephalus. The sum of the total outflows from the DA towards both the epicortical space and the spinal canal is represented by $V'_{B\,out}$.

2.2 The transport mechanisms

In order to simulate GVG and GCG conditions, a quantity of a dye or tracer substance soluble in the fluid is injected into compartment A or B respectively. We assume three possible mechanisms for the transportation and distribution of the test substance:

i) *bulk flow:* the substance perfuses the system and leaves it as a bolus in laminar and unidirectional flow. The contribution of CSF resorption to the total outflows is conceived as such a bulk flow.

ii) *ideal mixing:* the substance is distributed evenly throughout the system. We assume that, in each of the compartments, ideal mixing results in spontaneous and immediate distribution of any quantity of tracer substance entering one of the compartments by whatever route. At all times, therefore, each compartment contains a homogeneous tracer concentration.

iii) *backmixing flow:* this chemical engineering term denotes turbulent flows of dyed or tracered fluids, or solutions in which turbulence in the system spreads the substance in all directions, even against the main fluid current. *Therefore we assume, in pathological cases, a turbulent flow from the CVS to the DA, to which a backmixing effect is superimposed, generating the appearance of the pathological CVR between DA and CVS* [5].

2.3 Mathematical treatment of the model

2.3.1 Prerequisites and simplifications

The quantitative mathematical description of the hydrodynamic model starts with the formulation of assumptions and simplifications.

i) The volumes V_A and V_B and all CSF flows that occur are constant during the period of investigation. Consequently, the ratio of the volumes V_A and V_B

$$v_0 = V_A/V_B \tag{1 a}$$

and the ratios between each of the CSF flows occuring and the production flow $V'_{A\,in}$

$$v_i = V'_i/V'_{A\,in} \qquad (i = A\,out, AB, BA, B\,in, B\,out) \tag{1 b–f}$$

are also constant in time.

ii) There is conservation of fluid, *e. g.* due to the incompressibility of fluids, the total CSF production is equal to the total CSF resorption and outflow

$$V'_{A\,in} + V'_{B\,in} = V'_{A\,out} + V'_{B\,out}. \tag{2}$$

iii) For the same reason, the sums of all inflows to and outflows from each of the two compartments are equal. Therefore, the CVR V'_{BA} from the DA to the CVS is

$$V'_{BA} = V'_{AB} + V'_{A\,out} - V'_{A\,in}. \tag{3}$$

2.3.2 The differential equations for the tracer concentrations

The time behaviour of the tracer concentrations in the two compartments of the hydrodynamic model is quantified by two differential equations which are derived by applying to the model system the pro-

* Figs 1, 2, and 3 refer to case 3 in [5] and are reprinted with the permission of the publisher of Acta Neurochirurgica.

cedures used for the mathematical representation of either radioactive decay series [17–19], the kinetics of chemical reactions [20–22], or pharmacokinetics [21].

The time rates of change of the quantities involved in the process during a unit of time, *e. g.* the time derivatives of the number of nuclei, or, as the case may be, the amounts or concentrations of substances, are expressed in terms of those quantities remaining unchanged by the process. Usually, linear differential equations are obtained in this way, which are solved in accordance with the initial conditions of the process.

In the model, the tracer concentration changes I'_A and I'_B ($I'_i = dI_i/dt$; i = A, B) are related to the remaining tracer concentrations I_A and I_B in the compartments A and B. Depending on whether the tracered fluid is postulated to have been injected into A or B, two sets of solutions are obtained which mathematically represent the time behaviour of the tracer concentrations under, respectively, GVG or GCG conditions. For convenience, the solutions are normalized by dividing the GVG or GCG solution sets by the initial – and maximal – tracer concentrations I^0_A or I^0_B in the injected compartment A or B respectively. (Procedures and details in the Mathematical Appendix.)

2.3.3 Analysis of the solutions

Expressions for the following parameters are derived from the solutions, which are referred to as (A 7) and (A 8) of the Mathematical Appendix:

- the *initial slopes* (or gradients) *of the tracer concentrations, e. g.* the velocities of tracer concentration changes in A and B at the moment $t = 0$ of tracer injection (A 9, A 10),
- the *time* t_{max}, at which maximum tracer accumulation is expected in the non-injected compartment, *e. g.* B in GVG or A in GCG examinations, (A 11), and
- the *tracer concentrations* and the *concentration ratios at the time* t_{max} (A 13).

These parameters have been selected because, on the other hand, the numerical values of these quantities can likewise either be read directly or evaluated graphically from tracer concentration curves measured in real GVG or GCG examinations. (Methods and details in the Mathematical Appendix.)

3. Discussion and Conclusions

The attempt to describe a biological system as complex as CSF dynamics with the help of a technically based model required varying degrees of simplification and abstraction. Thus, the hydrodynamic model reflects neither the complex anatomical configuration of the CVS and DA, nor the physiological production and resorption processes in the walls. Pulsations and pressure variations are ignored as well, and two different CSF conduits between CVS and DA are assumed in the model instead of one anatomical duct.

On the other hand, the same physical principles of fluid mechanics are valid in every system involving fluids in motion. This means that both the simplified hydrodynamic model and even the most complex CSF flow system must obey the *basic principles of hydrodynamics*, and therefore should reveal the same mechanisms and phenomena.

3.1 Transport mechanisms

For that reason, the transport mechanisms assumed to occur in the hydrodynamic model are also anticipated, and in fact encountered, in CSF dynamics. Two of us have described the normal epicortical CSF circulation as a laminar bulk flow [12], and observed ideal mixing in the DA [4].

The theory and the kinematics of turbulent flows emphasize the concept that the pathological CVR from the DA to the CVS, observed in GCG examinations, is indeed an effect of a turbulent flow from CVS to DA, with a superimposed backmixing component.

In turbulent flows, vortices separate from the boundary layers between the walls of the system and the moving fluid [23–25]. Concomittant with the formation of eddies, a *reverse* flow occurs which – in particle-laden flows – gives the *appearence* of an upstream transfer of matter superimposed on the downstream fluid movement [25]. Therefore, a dye or tracer substance injected downstream into a system with turbulent flow can be convected in an upstream direction. The extent of this backmixing effect depends on system geometry and dimensions, curvature, pulsations and roughness of the walls, flux velocity, physical properties of the system and the fluid, temperature, pressure gradients, etc.

3.2 The time behaviour of the tracer concentrations

The transport mechanisms acting on the fluid in the hydrodynamic model change the tracer concentrations in time according to the formulae (A 7) and (A 8) in the Math. App. If appropriate numerical values are assigned to the volumes and fluid flows in these equations, the model can be adapted to any type of normal or pathological CSF flow system. Then the time behaviour of the tracer concentrations in the model can be compared to those observed in real GVG and GCG examinations.

3.2.1 GVG findings

3.2.1.1 Observations in real GVG

A subject *without CVR, i. e.* $V'_{BA} = 0$, displays a typical *isotope clearance process* in the CVS after ventricular tracer injection in GVG examinations. The amount of tracer initially administered is diluted by the continuous CSF production $V'_{A\,in}$, and fractions of tracer are steadily carried away by the physiological outflow V'_{AB} to the DA, and the ventricular resorption process $V'_{A\,out}$.

The total ventricular CSF efflux is balanced exactly by the CSF production $V'_{A\,in}$. The time course of the normalized tracer concentration I_A/I_A^0 in the CVS is an exponential which starts from the value 1 and decays according to

$$I_A/I_A^0 = \exp(-ft). \tag{4}$$

As the rapidity of any clearance process is determined by the ratio between total system outflow and system volume, the *frequency f of fluid renewal* [26] is

$$f = (V'_{AB} + V'_{A\,out})/V_A \tag{5 a}$$

or, with (3),

$$f = V'_{A\,in}/V_A. \tag{5 b}$$

From (4) follows that the semilogarithmic plot of tracer concentration versus time is a straight line with the slope f. As the CSF flow V'_{AB} from the CVS to the DA continuously transfers fractions of tracer towards the cisternal system, a tracer concentration is built up in the DA. Starting from the value zero, this tracer concentration attains a maximum value and then decreases slowly.

At the first glance, the pattern of the tracer concentration courses in cases *with CVR* resembles that in subjects without CVR. The fraction of tracer brought back from the DA to the CVS by the CVR V'_{BA} disturbs the evolution of tracer concentration in the CVS, so that the semilogarithmic plot of the tracer concentration versus time no longer results in a straight line. This indicates that the decay of the tracer concentration in the CVS is not singly exponential. Both the initial slope of the ventricular concentration change and the initial rise of the tracer concentration in the DA appear steeper than under normal conditions. Furthermore, the time needed to attain maximal tracer accumulation in the DA shifts towards shorter durations.

3.2.1.2 GVG response of the model

With appropriate coefficients, equation (A 7 a) degenerates to the clearance expression (4), if the backmixing flow $V'_{BA} = 0$. The frequency f of fluid renewal agrees with (5 a). It is equal to the initial slope (A 9 a) and shows that the initial tracer concentration change in the CVS is proportional to the total outflow $V'_{AB} + V'_{A\,out}$ from the CVS, which is balanced by the CSF production $V'_{A\,in}$ (5 b). A CSF production $V'_{B\,in}$ which may occur in the DA does not affect the tracer concentration in the CVS.

As the volume V_B of the DA is constant for a given CSF flow system, the initial velocity (A 9 b) of the tracer concentration development in the DA depends only on the afflux V'_{AB} to the DA from the CVS, which is smaller than, or at most, equal to $V'_{A\,in}$ (3).

In a system with backmixing flow, *i. e.* $V'_{BA} \neq 0$, the tracer concentration behaviour (A 7 a) becomes a linear combination of two different exponentials. Therefore, the semilogarithmic plot is not linear. However, the initial decrease of the tracer concentration in the CVS (A 9 a) is accelerated, because V'_{AB} is now greater than without backmixing flow. This follows from (3), since the difference $V'_{A\,in} - V'_{A\,out}$ remains unchanged. For the same reason, the increase of the tracer concentration in the DA (A 9 b) is also more rapid. Hence the tracer concentration in the DA attains maximum accumulation earlier.

3.2.1.3 Criterium for CSF production in the DA

GVG examinations of both CSF flow systems with or without CVR usually reveal that identical tracer concentrations in the CVS and DA occur at a certain time. At that moment, in typical plots of tracer concentrations versus time, the tracer concentration curve of the DA reaches, and exceeds the tracer concentration curve of the CVS, and then declines slowly towards zero.

The model allows equal values of tracer concentrations to occur in both CVS and DA at the calculated time t_{max} (A 11) of maximum tracer concentration in the DA, with the additional restriction that there is no CSF production in the DA. Only in this special case, *i. e.* if $V'_{B\,in} = 0$, the ratio (A 13 a) of the tracer concentrations in DA and CVS takes its maximum value 1. Otherwise it will be smaller than 1. Therefore, the relation (A 13 a) permits the interpretation of a crossing over of the tracer concentration curves of DA and CVS in GVG examinations, at the time of maximal tracer accumulation in the DA, as a *criterium for whether or not there is a CSF production $V'_{A\,in}$ in the DA.*

3.2.2 GCG findings

3.2.2.1 Observations in real GCG

The GCG of subjects *without CVR* indicates an isotope clearance process in the DA. Similar to the ventricular clearance observed in GVG, the initial tracer concentration in the DA decreases exponentially with a frequency of fluid renewal now determined by the total outflow $V'_{BA} + V'_{B\,out}$ from the DA, and the DA volume V_B. Also here, the outflow is compensated by the total afflux $V'_{AB} + V'_{B\,in}$ to the DA. Because there is no CVR, a tracer concentration in the CVS is not observed.

In pathological cases *with CVR*, the decrease of the initial concentration in the DA is faster and no longer a single exponential. Due to the CVR V'_{BA} from the DA to the CVS, a fraction of tracer is transferred towards the CVS against the normal CSF flow current V'_{AB} directed from the CVS to the DA.

Thus, starting from zero, a tracer concentration is built up in the CVS. It attains a relatively flat maximum and drops asymptotically towards the time axis.

3.2.2.2 GCG response of the model

The situation of GCG is described in the model by equations (A 8). Without backmixing flow, *i. e.* $V'_{BA} = 0$, the tracer concentration in the CVS (A 8 a) degenerates to zero throughout. The time behaviour of the tracer concentration in the DA (A 8 b) is reduced to a single exponential in which the frequency of fluid renewal is equal to the initial slope (A 10 b) and proportional to the total DA inflow $V'_{AB} + V'_{B\,in}$. In a model with backmixing flow, the initial decrease of the tracer concentration in the DA (A 10 b) is accelerated as V'_{AB} increases. The initial velocity of tracer concentration evolution in the CVS (A 10 a) is governed by the magnitude V'_{BA} of the CVR.

3.2.2.3 The backmixing factor

The flat time course of the tracer concentration in the CVS and its relatively low maximum value result from the circumstance that the fraction of tracer substance which the CVR V'_{BA} brings back to the CVS, is simultaneously diminished by the CSF flows $V'_{AB} + V'_{A\,out}$ leaving the CVS. The ratio r of these CSF *flows*

$$r = V'_{BA}/(V'_{AB} + V'_{A\,out}) \tag{6}$$

which is always lees than 1, is a measure for the degree of backmixing in a CSF flow system. We have introduced this ratio, multiplied by a factor 100, as a percentage, and called it *backmixing factor of the system* [5]. The model yields the same relation for the ratio between the *tracer concentrations* in the CVS and DA (A 13 b) at the time t_{max} (A 11), and thus offers a simple method for the numerical evaluation of backmixing factors. The values of the tracer concentrations in the CVS and DA at the time of maximal tracer accumulation in the CVS are read from the time plots, divided by another, and multiplied by 100.

3.2.3 Example

The upper parts of Figs 2 and 3 illustrate the typical time behaviour of the tracer concentrations in the CVS and DA of a patient (case 3 in [5]) as found in GCG and GVG examinations respectively. The patient's original curves are mounted together with the corresponding theoretical ones (lower parts of Figs 2 and 3), which have been calculated, and plotted, according to the model, with appropriate values for the CVS and DA volumes, and CSF flows inserted into (A 7) and (A 8). Further details are given in the section about practical applications.

3.3 Hydrodynamic principles

3.3.1 The time t_{max}

The model predicts maximal tracer accumulation in the DA after ventricular tracer injection (GVG) at a time t_{max} (A 11) which we can write in the form

$$t_{max} = F_t \cdot V_A / V'_{A\,in}\,. \tag{7}$$

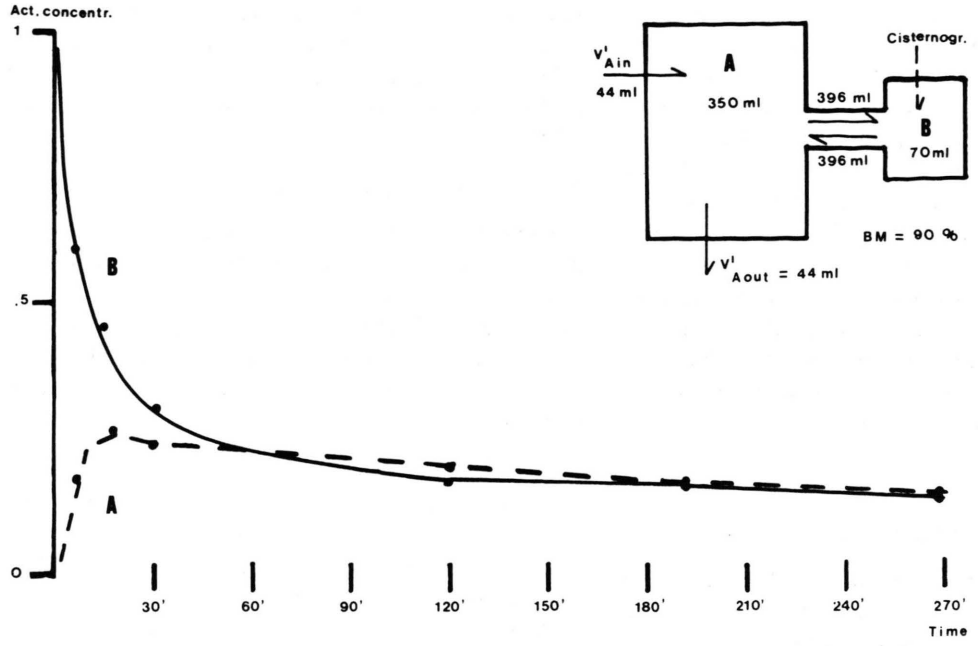

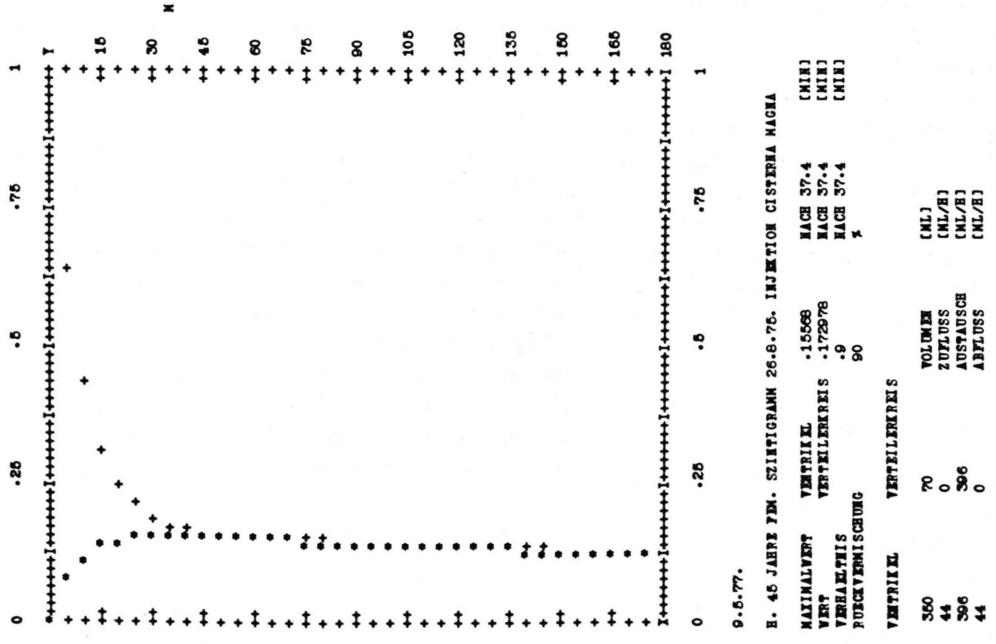

Fig. 2*. Example of a clinical case. Top: Time courses of tracer concentrations in DA (B) and CVS (A), measured by GCG. Bottom: Corresponding computer printout according to the model. The values are provided by GCG.

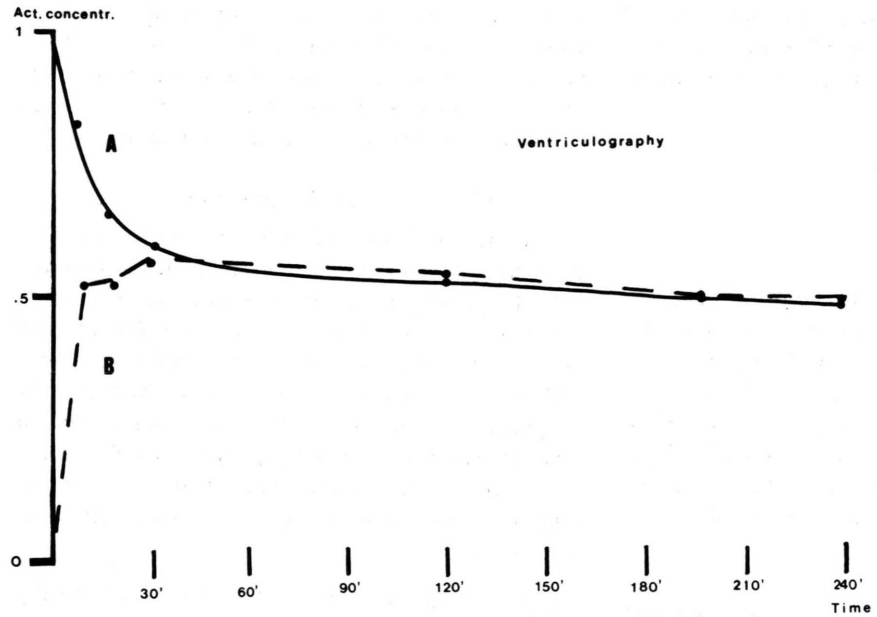

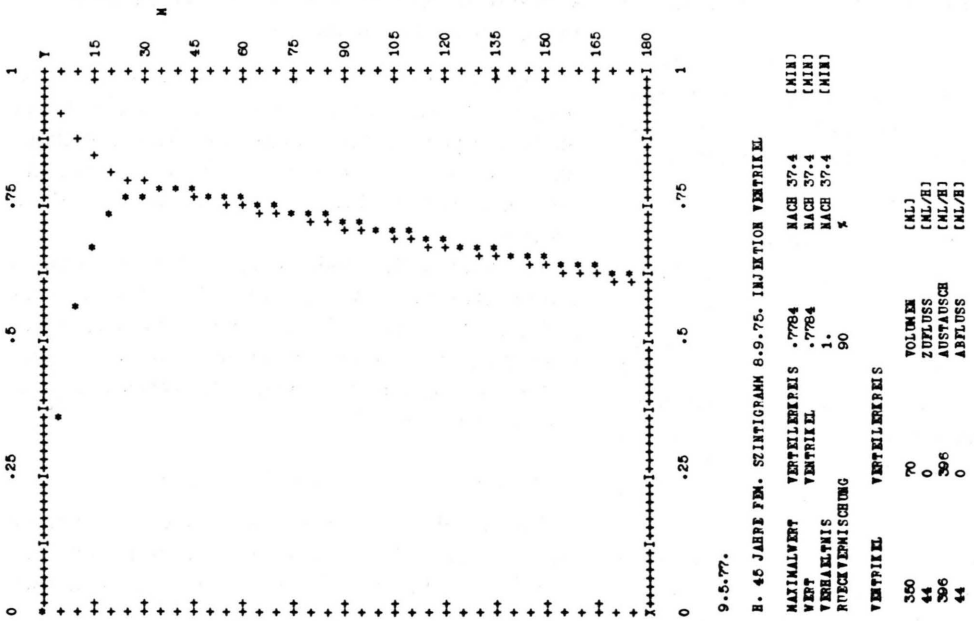

Fig. 3*. Same clinical case as in Fig. 2. Top: Time courses of tracer concentrations in CVS (A) and DA (B), measured by GVG. Bottom: Corresponding computer printout according to the model.

The identical expression results for the time of maximal tracer enrichment in the CVS after cisternal tracer instillation (GCG). (Details in the Math. App.)

3.3.1.1 The pool turnover time

The quotient

$$p = V_A / V'_{A\,in}$$

in relation (7) is the reciprocal of the frequency of fluid renewal (5 b), which rules the velocity of the tracer clearance process in the CVS observed in GVG examinations without CVR. The dimension of p is time. As the physical meaning of p is the time necessary to fill a recipient of the volume V_A by a constant fluid flow of the magnitude $V'_{A\,in}$, it is sometimes referred to as *pool turnover time* [26].

3.3.1.2 The system factor

The factor F_t in (7) is a non-dimensional function depending only on the volume and CSF flow *ratios* (1 a – e). It has a specific value for a given system with specific CSF flow conditions. Therefore we interprete it as a *system constant* or *system factor.* Beyond this, however, a system factor once calculated for a particular CSF flow system also applies to the entity of all systems with the same volume and flow ratios (1 a – e).

There is still another term which can be understood as a system factor. It is the common proportionality constant which can be factored out from the expressions derived for the tracer concentrations at the time t_{max} (see Math. App.).

3.3.2 The principle of dynamic similitude

We consider the occurence of system factors in the dynamics of CSF flow as a consequence of the *principle of dynamic similitude.* This general concept of fluid dynamics forms the basis of the theory of models, which permits the investigation of complex flow patterns of a particular flow system by making experiments on a geometrically similar system differing from the original or prototype system only in size [24].

The theoretical model of CSF dynamics reduces the stringent condition of exact geometrical similarity in form and dimensions of systems in comparison to the demand of more proportionality between volumes and CSF flow magnitude, respectively. If, *e. g.*, the volume and/or the CSF flow values of a system S 2 can be obtained by multiplying the volume and/or flow values of a system S 1 by numerical constants m and/or n respectively, then the system factors of both systems are identical, as the ratios (1 a – e) do not change their values.

3.3.3 Similarity law of CSF flow systems

The fact that entities of CSF flow systems are represented by one common system factor, together with the principle of dynamic similitude, leads us to postulate the existence of a *similarity law of CSF flow systems.* The meaning of this law is, that two CSF systems which differ one from another only by proportionality factors referring to volumes and/or CSF flows, reveal similar hydrodynamic behaviour.

A conceivable consequence of the concept of similarity may facilitate the analysis of CSF flow systems by

i) providing for a *classification* of the theoretically infinite number of possible systems according to their system factors and pool turnover times, and

ii) reducing the *comparison* of systems with the same (in practise similar) system factors to the comparison of their pool turnover times and vice versa.

4. Practical applications of the theoretical model to problems of CSF dynamics

Apart from the theoretical implications and aspects of CSF dynamics, we see the practical value of the hydrodynamic model mainly in offering methods for the *quantitative analysis of CSF flow systems,* and the *simulation of GVG and GCG conditions* in these systems.

According to the model, every CSF flow system is completely defined by eight variables – two volumes and six CSF flows. The parameters pool turnover time, time of maximum tracer accumulation, system factor, and backmixing factor, are likewise expressions in these variables.

4.1 Quantitative evaluation of CSF flows

Whereas the volumes of the CVS and DA can be estimated from frontal and lateral radionuclide images [5, 6], the six CSF flows occur as unknown variables. Besides the equilibrium condition between CSF production and elimination in the system (2), and the balance between the CSF flows into and out of each compartment (3), the model yields a total of

six expressions which relate the numerical values of the ratios (A 13) of the tracer concentrations at the time t_{max} and their initial slopes (A 9, 10) to CSF flows and volumes. Provided that the tracer concentration curves of GVG or GCG examinations have been recorded with a sufficiently great time resolution, the numerical values of the initial slopes and the ratios of the tracer concentrations can be evaluated from the corresponding GVG and GCG tracer concentration curves, and substituted into the left sides of (A 9), (A 10), and (A 13).

Four numerical values for the initial slopes of the tracer concentrations are available, if both GVG and GCG examinations have been performed. In this case, the four relations (A 9 a, b), (A 10 a, b), together with (2) and (3), define a system of six independent linear equations for the six unknown CSF flows. The solution of this problem is unique. Usually, only data of one examination – preferably GCG – are present. These are (2) and (3), with the initial slopes (A 10 a, b) and the backmixing factor (6). (In the case of GVG, equations (A 9 a, b) and the tracer concentration ratio (A 13 a) at the time t_{max} are used.)

In both situations three CSF flows can be evaluated directly leaving only two equations for three variables. Then, one variable is free and chosen arbitrarily, so that the remaining variables can be calculated. The estimation of the free variable is tested by inserting all CSF flows into the expression (A 11) for the time t_{max}. The calculated theoretical value for t_{max} is compared with that value measured in the real tracer concentration curve. Unless both values agree sufficiently, the free variable is altered, and the procedure repeated. These calculations can be performed automatically with a programmable pocket or desktop calculator, or a computer program.

4.2 Simulation of GVG and GCG

Equations (A 7) and (A 8) enable one to calculate the time response of the tracer concentrations to GVG and GCG in any conceivable CSF flow system with the only restriction that the CSF flow system satisfies the continuity equations (2) and (3).

The calculations to simulate GVG or GCG conditions in a particular CSF system can also principically be performed by a programmable pocket or desktop calculator. A digital computer, however, is a more convenient tool for this purpose. It performs the calculations much faster, and provides – with an appropriate programme – for automatic subsequent plots of the tracer concentrations in CVS and DA versus time. For this purpose we use a Hewlett-Packard 2116 C-computer, with 8 k memory and a teletype, and a CSF analysis programme package written in BASIC. This configuration produces the computer plots of the temporal evolution of tracer concentrations in the patient (lower parts of Figs 2 and 3).

The programme processes data for CVS and DA volumes and CSF flows, which have either been measured in scintigraphic studies, or theoretically assumed, and enumerates the values of t_{max}, pool turnover time, system factor, and backmixing factor. The influence of alterations of the backmixing factor or pool turnover time on a system can similarily be studied, because one program uses those variables as inputs and calculates the CSF flows instead.

4.3 Example

The history of the generation of Figs 2 and 3 demonstrates an advantage of the simulation facilities inherent to the model. A 45 year old female patient suffering from a subarachnoid haemorrhage and secondary development of hydrocephalus, was first submitted to GCG. The resulting temporal evolution of isotope concentrations in the DA (B) and CVS (A) are displayed in the upper half of Fig. 2. Whereas the CVS and DA volumes could have been evaluated from the digital scintigrams, we had to estimate the CSF production $V'_{A\,in}$, the transependymal resorption $V'_{A\,out}$, and the backmixing factor, as the model was not yet fully developed for the direct evaluation of CSF flows at that time. By experience [16], the CSF production within the DA, and the resorption or outflow from the DA could be neglected in this case.

The computer program simulates GCG in this system with the following data: $V_A = 350$ [ml], $V_B = 70$ [ml], $V'_{A\,in} = V'_{A\,out} = 44$ [ml/h], $V'_{B\,in} = V'_{B\,out} = 0$, backmixing factor $r = 90\%$, and calculates a common result for both the CSF flow from the CVS to the DA, and the CVR. The value $V'_{A\,B} = V'_{B\,A} = 396$ [ml/h] is considerably large, and indicates a highly disturbed CSF flow pattern.

With the same set of data we then simulated GVG conditions in this system (lower part of Fig. 3). A real GVG investigation was performed two weeks

later and yielded the tracer concentration curves in the upper part of Fig. 3. The curves of the real tracer concentrations in the CVS (A) and DA (B) correspond to the previous theoretical printout.

So, with the data known, evaluated, or estimated from clinical examinations, the calculation according to the model can confirm the scintigraphic findings and – in some cases – *save patients from a further investigation.* As a consequence, we recommand against GVG in most cases and are satisfied with a GVG simulation with data evaluated from GCG examinations. In addition, the comparison of theoretically simulated CSF volume and flow conditions with unclear or unusual clinical findings can give helpful aids in diagnostics.

4.4 Normal and pathological system factors

As GCG, and especially GVG, require delicate procedures to the human body, these examinations are only performed upon the most stringent indications. Therefore in a *normal* human subject, the time t_{max}, at which maximum tracer concentration would be expected in the DA after ventricular tracer injection, withdraws from direct measurement by GVG. Without t_{max}, the system factor F_t of a normal CSF flow system cannot be calculated either.

The *normal values* of both parameters, however, can be evaluated theoretically. Inserting the normal values [16]

$$V_A = 45 \pm 5\,[\text{ml}], \quad V_B = 60 \pm 5\,[\text{ml}],$$

$V'_{A\,in} = V'_{AB} = V'_{B\,out} = 21 \pm 2\,[\text{ml/h}]$ – the other CSF flows are zero – reduces equation (A 11) to

$$t_{max\ norm} = (V_A/V'_{A\,in}) \cdot (V_B/(V_A - V_B)) \cdot \ln (V_A/V_B) \quad (8)$$

and yields the norm values

$$t_{max\ norm} = (2.35 \pm .27)\,[\text{h}] \quad (9)$$

and a system factor

$$F_{t\ norm} = (1.15 \pm .08). \quad (10)$$

In all our clinical cases [16] we have encountered system factors which differ from the norm value of 1.15 by one order of magnitude or even more. (The patient of Figs 2 and 3 has a system factor of .08.) We think, that it may be possible to assign either different syndromes to different F_t values or to distinguish different stages in the development of a disease by means of altered system factors.

On the base of our clinical material, we have recently attempted to classify several stages in the development of the hydrocephalic syndrome [16]. As criteria we used clinical findings, scintigraphic results, and the model parameters t_{max} and backmixing factor. Preliminary calculations performed now support the assumption that the system factors stepwisely decrease with each evolutionary stage in the development towards a chronical hydrocephalic syndrome. This provisional observation is based on a sample of only 18 cases. With a larger sample of patients, we hope, in the future, to confirm this correlation with sufficient statistical confidence.

4.5 Final remarks

The derivation of the theoretical model of CSF flow dynamics and its applications to specific clinical problems has – in our opinion – enhanced the potential of scintigraphic examinations by providing for a facility to extract quantitative informations from GVG and GCG records which originally have been only semiquantitative examinations. Therefore we recognize in our model a key to better understanding of the complex processes of CSF dynamics in the human central nervous system, and a base for further promising research in this field. For the deduction of this model we have used considerations, assumptions, and mathematical procedures which are customary in a broad range of scientific applications. We are convinced that our method is not restricted to the special case of CSF flow dynamics. We believe that in a similar way numerous processes may be treated and analysed in which substances, pharmaceuticals, enzymes, or hormones are accumulated and eliminated simultaneously, or undergo metabolic or chemical reactions. In particular we expect the similarity law and the concept of system factors also to apply to other physiological, pharmacokinetical, biochemical, and endocrinological processes.

Furthermore, the model can be expanded to include the description of processes in which periodical perturbations are superimposed to or interfere with the processes to be analysed. The situation of such an external periodical perturbation is represented, in the mathematical formalism, by an additional periodical term in equation (A 6). With this expansion, the model is able to take into account the effects of heartbeat, breathing, or other periodical events, on particular processes.

5. Mathematical Appendix

5.1 The initial conditions

The injection of a quantity m_0 of a radiotracer substance into either compartment A or B (Fig. 1) of the hydrodynamic model system at the time $t_0 = 0$ builds up the initial tracer concentrations I_A^0 and I_B^0 in the volumes V_A and V_B respectively, and defines the initial conditions

$$I_A^0 = m_0/V_A\,, \quad I_B^0 = 0 \tag{A 1 a}$$

for tracer application in compartment A (GVG), and

$$I_A^0 = 0\,, \quad I_B^0 = m_0/V_B \tag{A 1 b}$$

for tracer application in the compartment B (GCG) respectively.

5.2 The differential equation

At a certain time t, let the amounts of tracer substance in the compartments A and B be m_A and m_B respectively, causing tracer concentrations

$$I_A = m_A/V_A \quad \text{and} \quad I_B = m_B/V_B$$

respectively.

In the time interval between t and $t + \mathrm{d}t$, the fraction $m_B \cdot (V'_{BA} \cdot \mathrm{d}t)/V_B$ is removed from the tracer amount m_B in the volume V_B and transported into compartment A by the constant flow V'_{BA}. Simultaneously, the fractions

$$m_A \cdot (V'_{AB} \cdot \mathrm{d}t)/V_A \quad \text{and} \quad m_A \cdot (V'_{A\,out} \cdot \mathrm{d}t)/V_A$$

leave the volume V_A via the constant flows V'_{AB} and $V'_{A\,out}$. Hence, the net change $\mathrm{d}m_A$ of the amount of tracer substance in A during the time interval between t and $t + \mathrm{d}t$ is

$$\mathrm{d}m_A = m_B \cdot (V'_{BA} \cdot \mathrm{d}t)/V_B - m_A \cdot (V'_{AB} \cdot \mathrm{d}t + V'_{A\,out} \cdot \mathrm{d}t)/V_A\,.$$

Inserting $\mathrm{d}m_A = \mathrm{d}(V_A \cdot I_A) = V_A \cdot \mathrm{d}I_A$ and dividing both sides of the expression for $\mathrm{d}m_A$ by the differential $\mathrm{d}t$ leads to a differential equation for the rate of change $I'_A = \mathrm{d}I_A/\mathrm{d}t$ of the tracer concentration I_A in the volume V_A

$$V_A \cdot I'_A = V'_{BA} \cdot I_B - (V'_{AB} + V'_{A\,out}) \cdot I_A\,. \tag{A 2 a}$$

The differential equation for the tracer concentration I_B in the compartment B is obtained similarily:

$$V_B \cdot I'_B = V'_{AB} \cdot I_A - (V'_{BA} + V'_{B\,out}) \cdot I_B\,. \tag{A 2 b}$$

With the abbreviations

$$b = (V'_{AB} \cdot (V_A + V_B) + V_A \cdot V'_{B\,in} + V_B \cdot V'_{A\,out})/(2 \cdot V_A \cdot V_B)\,, \tag{A 3}$$

$$\omega_0^2 = (V'_{AB} \cdot (V'_{A\,in} + V'_{B\,in}) + V'_{B\,in} \cdot V'_{A\,out})/(V_A \cdot V_B)\,, \tag{A 4}$$

and

$$R = \sqrt{b^2 - \omega_0^2}\,, \tag{A 5}$$

the differential equation system (A 2 a, b) is transformed into a second order differential equation, an *oscillation equation*

$$I'' + 2 \cdot b \cdot I' + \omega_0^2 \cdot I = 0\,. \tag{A 6}$$

Equation (A 6) results for both the tracer concentrations I_A and I_B.

5.3 The solutions of the differential equation

The initial conditions (A 1 a, b) yield two different sets of two solutions each, describing the time dependence of the tracer concentrations I_A and I_B in both compartments A and B under GVG and GCG conditions respectively. For convenience, a *normalization* with respect to the initial tracer concentration in the injected compartment is performed by dividing the GVG solution set by I_A^0 and the GCG equations by I_B^0. The *normalized tracer concentrations* in the volumes V_A and V_B are

$$I_A/I_A^0 = C_A^- \cdot \exp(-(b - R)\,t) + C_A^+ \cdot \exp(-(b + R)\,t) \tag{A 7 a}$$

$$I_B/I_A^0 = V'_{AB} \cdot (\exp(-(b - R)\,t) - \exp(-(b + R)\,t))/(2\,R\,V_B) \tag{A 7 b}$$

with

$$C_A^{\pm} = \mp\,(V'_{AB} + V'_{B\,in} - V_B \cdot (b \pm R))/(2\,R\,V_B) \tag{A 7 c}$$

for tracer application in the compartment A (GVG), and

$$I_A/I_B^0 = V'_{BA}\,(\exp(-(b - R)\,t) - \exp(-(b + R)\,t))/(2\,R\,V_A) \tag{A 8 a}$$

$$I_B/I_B^0 = C_B^- \cdot \exp(-(b - R)\,t) + C_B^+ \cdot \exp(-(b + R)\,t) \tag{A 8 b}$$

with

$$C_B^{\pm} = \mp\,(V'_{AB} + V'_{A\,out} - V_A \cdot (b \pm R))/(2\,R\,V_A) \tag{A 8 c}$$

for tracer application in the compartment B (GCG).

5.4 Analysis of the solutions

The solutions (A 7), (A 8) are differentiated with respect to time. Inserting $t = 0$ into the time derivatives of the solutions, leads to relations between the initial slopes of the normalized tracer concentration curves, and the CSF flows and volumes.

5.4.1 The initial slopes are

$$(\mathrm{d}(I_A/I_A^0)/\mathrm{d}t)_{t=0} = -(V'_{AB} + V'_{A\,out})/V_A \quad \text{(A 9a)}$$

and

$$(\mathrm{d}(I_B/I_A^0)/\mathrm{d}t)_{t=0} = V'_{BA}/V_B \quad \text{(A 9b)}$$

for tracer application in the compartment A (GVG), and

$$(\mathrm{d}(I_A/I_B^0)/\mathrm{d}t)_{t=0} = V'_{BA}/V_A \quad \text{(A 10a)}$$

and

$$(\mathrm{d}(I_B/I_B^0)/\mathrm{d}t)_{t=0} = -(V'_{AB} + V'_{B\,in})/V_B \quad \text{(A 10b)}$$

for tracer application in the compartment B (GCG).

5.4.2 The time of maximum tracer accumulation

Setting the time derivative of (A 7b) equal zero yields the time

$$t_{max} = (\ln((b+R)/(b-R)))/(2R)\,, \quad \text{(A 11)}$$

for which maximum tracer accumulation is expected in the non-injected compartment B after tracer application in A (GVG). The same expression results from (A 8a) for the time of maximal tracer concentration in compartment A after tracer application in B (GCG).

Inserting (A 3–5) and (1 a–e) into (A 11) allows to factor out the quotient $V_A/V'_{A\,in}$ so that (A 11) can be rewritten as

$$t_{max} = F_t\,(v_0,\ v_{AB},\ v_{A\,out},\ v_{B\,in},\ v_{B\,out}) \cdot V_A/V'_{A\,in}. \quad \text{(A 12)}$$

The factor F_t is a function of the volume and flow ratios (1 a–e) only. Its implications for the CSF dynamics can be discussed, in the main text, without the knowledge of its explicite expression.

5.4.1 The tracer concentrations at the time t_{max}

Insertion of (A 11) into (A 7), (A 8) yields the *ratios of the tracer concentrations* at the time t_{max} for GVG and GCG examinations respectively. We obtain

$$(I_B/I_A)_{t=t_{max}} = V'_{AB}/(V'_{AB} + V'_{B\,in}) \quad \text{(A 13a)}$$

for tracer application in A (GVG), and

$$(I_A/I_B)_{t=t_{max}} = V'_{BA}/(V'_{AB} + V'_{A\,out}) \quad \text{(A 13b)}$$

for tracer application in B (GCG).

Similar to the representation of t_{max} in (A 12), the *tracer concentrations* at the time t_{max} can be rewritten in terms of the volume and flow ratios (1 a–e). The four expressions both for GVG and GCG conditions can be resolved in simple sums and products of the ratios (1 a–e), and a common proportionality factor. Like F_t in (A 12), this factor is a function of the volume and flow ratios (1 a–e) only, with analogous implications for CSF dynamics.

[1] R. N. Beck, Nuclear Medicine (H. N. Wagner jr., ed.), Chapter 2, Hospital Practice Publishing Co., New York 1975.
[2] H. O. Anger, Nuclear Medicine (H. N. Wagner jr., ed.), Chapter 3, Hospital Practice Publishing Co., New York 1975.
[3] H. N. Wagner and T. K. Natarajan, Nuclear Medicine (H. N. Wagner jr., ed.), Chapter 4, Hospital Practice Publishing Co., New York 1975.
[4] A. Palma and T. Kolberg, Acta Neurochir. **36,** 9–28 (1977).
[5] A. Palma, T. Kolberg, W. Entzian, A. Palma, and R. Wüst, Acta Neurochir. **43,** 19–50 (1978).
[6] M. Akerman, G. de Tovar, and G. Guiot, Cisternography and Hydrocephalus (J. C. Harbert, ed.), Chapter 39, Ch. C. Thomas, Springfield, Ill. 1972.
[7] G. Di Chiro, Acta Radiol. (Diagn.) (Stockh.) **5,** 988–1002 (1966).
[8] G. Di Chiro, Nuclear Medicine (H. N. Wagner jr., ed.), Chapter 10, Hospital Practice Publishing Co., New York 1975.
[9] M. Pollay, Cisternography and Hydrocephalus (J. C. Harbert, ed.), Chapter 2, Ch. C. Thomas, Springfield, Ill. 1972.
[10] O. Sato and E. A. Bering, Brain and Nerve **19,** 883–885 (1967).
[11] W. H. Oldendorf, Progress in Nuclear Medicine, **Vol. 1,** (E. D. Potchen and V. R. McCready, eds.), pp. 336–358, S. Karger, Basel 1972.
[12] T. Kolberg and A. Palma, Acta Neurochir. **38,** 1–12 (1977).
[13] A. Palma, T. Kolberg, W. Entzian, and A. Palma, Lumbar Disc, Adult Hydrocephalus. Advances in Neurosurgery, **Vol. 4,** (R. Wüllenweber, M. Brock, J. Hamer, M. Klinger, and O. Spoerri, eds.), pp. 137–143, Springer-Verlag, Berlin-Heidelberg-New York 1977.

[14] M. Akerman, G. de Tovar, and G. Guiot, Cisternography and Hydrocephalus (J. C. Harbert, ed.), Chapter 22, Ch. C. Thomas, Springfield, Ill. 1972.
[15] E. R. Heinz and D. O. Davis, Cisternography and Hydrocephalus (J. C. Harbert, ed.), Chapter 17, Ch. C. Thomas, Springfield, Ill. 1972.
[16] A. Palma, T. Kolberg, R. Wüst, and W. Entzian, Acta Neurochir. **45,** 53–88 (1978).
[17] E. Rutherford, Radio-Activity, University Press, Cambridge 1904.
[18] E. Rutherford and F. Soddy, Phil. Mag. Ser. 6, **Vol. 5,** 576–591 (1903).
[19] H. Bateman, Proc. Cambridge Phil. Soc. **15,** 423–427 (1910).
[20] W. W. Kafarow, Kybernetische Methoden in der Chemie und chemischen Technologie, Verlag Chemie, Weinheim 1971.
[21] H. Röpke and J. Riemann, Analogcomputer in Chemie und Biologie, Springer-Verlag, Berlin-Heidelberg-New York 1969.
[22] V. A. Harcourt and W. Esson, Phil. Trans. Roy. Soc. **156,** 193–221 (1866).
[23] P. Bradshaw, Turbulence (P. Bradshaw, ed.), Chapter 1, Springer-Verlag, Berlin-Heidelberg-New York 1976.
[24] J. W. Daily and D. R. F. Harleman, Fluid Dynamics, Addison-Wesley Publishing Co., Reading, Mass. 1966.
[25] L. Prandtl, K. Oswatitsch, and K. Wieghardt, Führer durch die Strömungslehre, F. Vieweg + Sohn, Braunschweig 1969.
[26] H. G. Knoetgen, G. F. Fueger, and G. Gell, Cisternography and Hydrocephalus (J. C. Harbert, ed.), Chapter 42, Ch. C. Thomas, Springfield, Ill. 1972.